Acta Crystallographica Section B
Structural Science
ISSN 0108-7681

The application of cluster analysis to identify conformational preferences in enones and enimines from crystal structural data

Anna Collins,*‡ Gordon Barr, Wei Dong, Christopher J. Gilmore, Derek S. Middlemiss, Andrew Parkin and Chick C. Wilson

WestCHEM, Department of Chemistry, University of Glasgow, Glasgow G12 8QQ, Scotland

‡ Now at School of Chemistry, University of Edinburgh, West Mains Road, Edinburgh EH9 3JJ, Scotland.

Correspondence e-mail: annac@chem.gla.ac.uk

Received 21 November 2006
Accepted 9 February 2007

Cluster analysis can be an effective tool for analysing large quantities of data. Here it has been applied to the conformational analysis of enones and enimines in the crystalline solid state, using structural information mined from the Cambridge Structural Database. The forms that are common in the gaseous state and in solution are already known from spectroscopic studies. These forms are also found to be the most common conformations observed in the solid state; however, the clustering method highlights those structures that do not conform to the expected geometries. The study is supported by *ab initio* gas phase calculations on simple enone and enimine fragments.

1. Introduction

The conformational analysis of enones and enimines is commonly based on spectroscopic studies, by NMR (Abraham & Lucas, 1988), IR or Raman (Oelichmann *et al.*, 1982*a*), or theoretical calculations (Wang *et al.*, 2005). It is principally of interest as it relates to the conformations of products of subsequent reactions (Childs *et al.*, 1988) and processes such as the enone–enolate equilibrium (Chamberlin & Reich, 1985). Most of these studies have been undertaken on the conformations in the solution or gas phase; we are interested in the conformations adopted in the solid state and how these relate to the solution-phase and gas-phase structures. This type of information is important for scientists engaged in drug or materials discovery, for whom crystal structure data is incredibly useful for modelling purposes.

The configuration of the fragment is usually considered to be described fully by two principal components, the configuration about the double bond, C2═C3 (see Fig. 1), which can be *cis* or *trans*, and the conformation about the single bond C3—C4. This can be described by the dihedral angle (φ) between the two rigid components (C1, C2 and C3, and C4, C5 and O/N6). It is termed s-*trans* for $\varphi = 180^\circ$ or s-*cis* for $\varphi = 0^\circ$ (Oelichmann *et al.*, 1982*b*). Previous spectroscopic and theoretical studies, and chemical intuition, indicate that the enone or enimine fragment will tend to be planar. By studying this fragment in the crystalline environment using cluster analysis it should be possible to see if these descriptions also hold true in the solid state. If molecules found in the crystalline solid state conform to these expected geometries, then clusters based on fragment geometry should be very well defined; this will also mean that fragments whose geometries are in any way unusual, either through error or arising from some feature of the structure as a whole, should be easily identifiable (Barr *et al.*, 2005). This should also allow any other factors that contribute to the structural geometry to be identified.

The study of conformations of particular functional groups or motifs in the solid state has been facilitated by the availability of crystallographic databases such as the Cambridge Structural Database (CSD; Allen, 2002). The application of cluster analysis to large datasets allows for rapid data processing and the use of suitable visualization tools promotes the observation of anomalous conformations in the bulk data, which may be more difficult to notice by examination of the data for individual structures. Here, cluster analysis has been applied to enones and enimines extracted from the CSD. Analysis has been performed using the freely distributed *dSNAP* software (Barr *et al.*, 2005), in addition to the CCDC programs *ConQuest* and *Mercury* (Bruno *et al.*, 2002).

To back up the cluster-analysis results, we have also carried out *ab initio* theoretical-energy calculations for the gas-phase structure of pent-2-ene-4-one and the corresponding enimine, 4-penten-2-imine. This allows us to assess whether the ratios in which the different geometries are observed in the crystalline solid state are consistent with their calculated relative energies in the gas phase.

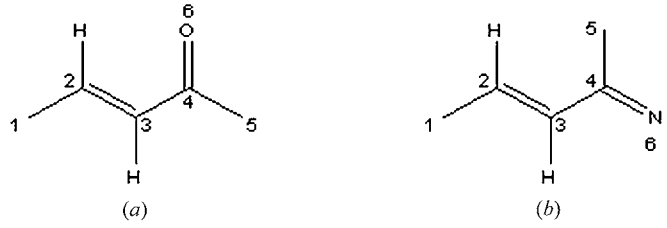

Figure 1
(*a*) The enone and (*b*) enimine search fragments, showing the atom-numbering scheme. The enone is drawn in the *trans* s-*cis* form and the enimine in the *trans* s-*trans* form.

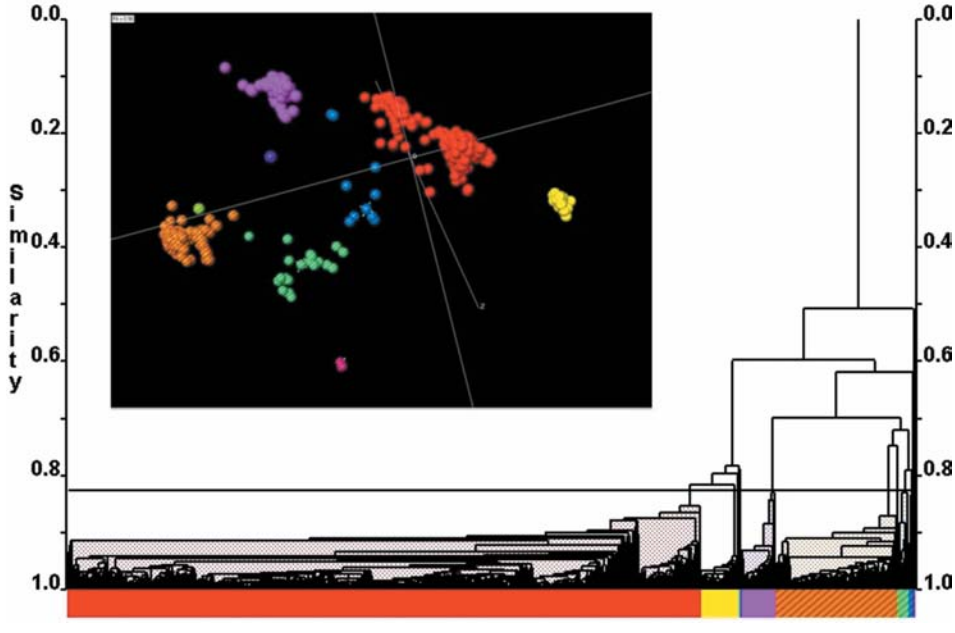

Figure 2
Dendrogram and MMDS plot (inset) for the enone search fragment.

2. Experimental

The clustering method has been fully described elsewhere (Barr *et al.*, 2005). A chemical search fragment or fragments are defined and a scan of the CSD is initiated using *ConQuest*, resulting in a list of crystal structures, or hits. A hit structure may contain more than one instance of the fragment(s) that were searched for (for example, structures with $Z' > 1$), so the resulting number of fragments used in cluster analysis is generally larger than the number of hits.

For every fragment all the interatomic distances (bonded and non-bonded, and not just those involving chemical bonds or nearest-neighbour contacts) and angles are extracted. The number of geometric parameters is thus equal to $(l/2)(l-1) + (l/2)(l-1)(l-2) = l/2(l-1)^2$, where l is the number of atoms. This results in some redundancy, as the fragment geometry is completely characterized by the distances alone, but in our experience the use of distances and angles together has proved to be optimal in practice, and more powerful than the use of distances alone. Although it would be possible to include torsion angles as well, there seems to be little benefit in doing so; the geometry is sufficiently characterized by the distances and angles. The search results are exported, along with the relevant *ConQuest* files, into *dSNAP* in the form of a data matrix, **x**, comprising n rows and m columns (where n is the number of fragments and m is the number of geometric parameters). The data matrix is then converted into distance and similarity matrices and these are now used to generate a metric multidimensional scaling (MMDS) representation of the data and a dendrogram.

The dendrogram takes the form of a tree with each fragment represented by one of the boxes arranged at the bottom of the plot (see Fig. 2). Boxes are joined by a series of lines linking fragments together according to the calculated similarity between each connected branch. The horizontal lines connecting the fragments are known as tie-bars. The vertical scale represents geometric similarity. Structures joined by tie-bars at the top of the dendrogram (at a similarity of zero) are completely different. Structures joined by tie-bars at a high similarity value (at the bottom of the dendrogram) are very similar. A cut-level is imposed at a specified similarity. Fragments which are connected by tie-bars at a similarity with a higher value form a cluster. Thus, the choice of cut-level determines the number of clusters that are observed. The choice of cut-level is non-trivial; the program estimates it using a principal-components analysis of

the distance matrix (which includes distance and angle information) with the condition that the principal components explain 95% of the variability of the data.

Metric multidimensional scaling (MMDS) is also a valuable tool in establishing the number of clusters. In an MMDS plot, each fragment is represented by a sphere in a three-dimensional cube. The closer that the two spheres are in the plot, the more similar their geometries, *i.e.* MMDS preserves the distance matrix. Applying the colours of the clusters for a given cut-level in the dendrogram to the MMDS plot allows the choice of cut-level to be assessed. Ideally, clusters should form discrete groups that are well distanced from any of the other fragments in the plot. We can assess how well the MMDS plot reproduces the original distance matrix by calculating the mean of the Spearman and Pearson correlation coefficients between the original matrix and that calculated from the MMDS method. Values greater than 0.8 are not uncommon and are indicative of a good fit and thus a high degree of confidence in the MMDS representation. The mean correlation is called the fit in this paper.

In this paper, the clustering levels have been chosen to highlight the major differences between structures. Further detail, where appropriate, has been elucidated through re-clustering selected fragments. Initially, the results of each clustering classification are described, followed by a discussion of their chemical significance.

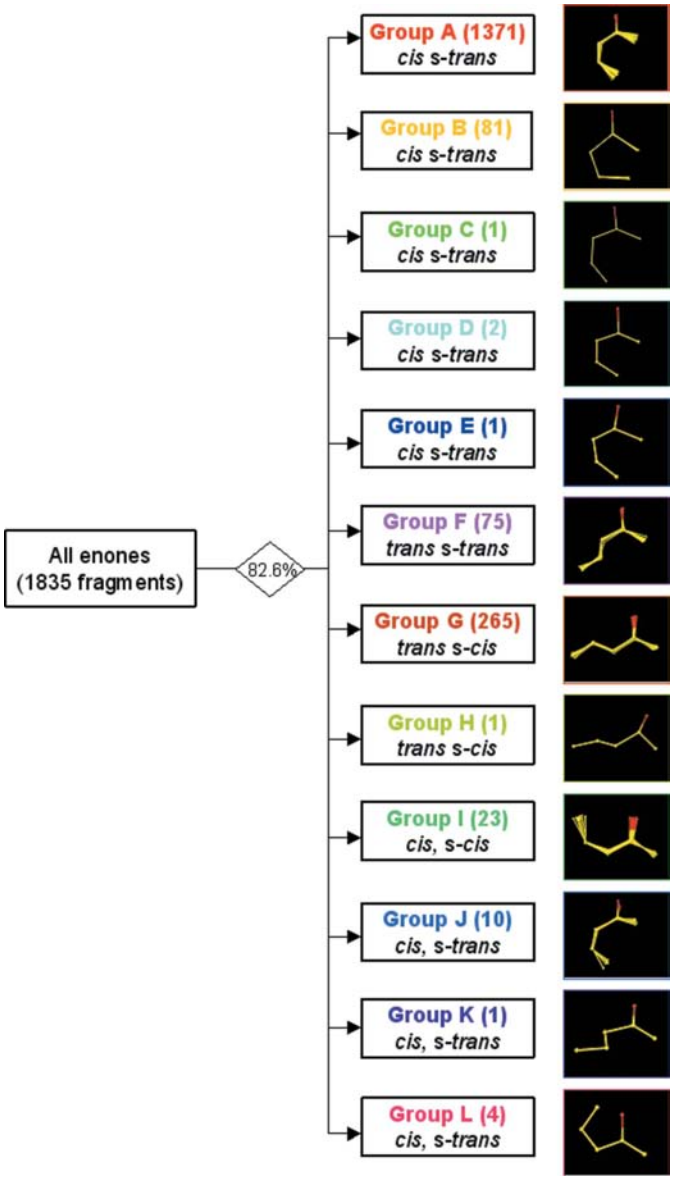

Figure 3
Decision tree describing the distribution of the enone geometries.

3. Enone fragment clustering

The fragment in Fig. 1(*a*) was defined. The cyclicity of all bonds was initially undefined. The CSD search resulted in 1260 hit crystal structures, containing 1835 instances of the search fragments, which were used in the subsequent analysis. At a cluster cut level of 0.826 there are 12 clusters, A to L. These clusters are well separated in the MMDS plots, with a fit of 0.98 (see Fig. 2).

Groups A to E contain structures that are *cis* s-*trans*. In group A (1371 fragments), the carbon backbone forms part of a six- or seven-membered ring. Group B (81 fragments) corresponds to structures where the carbon backbone forms a five-membered ring. Groups C (one fragment), D (two fragments) and E (one fragment) represent anomalous structures. In groups D and E the carbon backbone again forms part of a six-membered ring. In Group D C4 is out of the plane of the other atoms, resulting in geometric distortions, notably in the length of the C4═O6 double bond. In group E the geometry is distorted by the presence of an epoxide group on the six-membered ring. The enone is part of a seven-membered ring in group C which appears slightly distorted. Group F (75 fragments) consists of structures where the enone is of a planar *trans* s-*trans* conformation. Group G (265 fragments) and H (one fragment) both contain fragments with a *trans* s-*cis* geometry. Group H contains a structure (BETNIY) where the C1—C2—C3 angle is particularly large and the C4—O6 bond is particularly short. Group I enones (23 fragments) are of a planar *cis* s-*cis* geometry. Group J (ten fragments) consists of enones with a *cis* double bond. The atoms in the group are non-coplanar, making assignment of the conformation of the C3—C4 single bond problematic. The single enone fragment that forms group K (ZZZGUC01) is of the *trans* s-*trans* conformation. It has a C1—C2—C3 angle of 90.2°, while all other the fragments are fairly evenly distributed in the range 106–142°; it also has particularly long C1—C2 and C3—C4 bonds (1.826 and 1.743 Å, respectively). This structure is likely to be in error. Group L (four fragments) contains fragments of a *cis* s-*cis* conformation. The O atom forms part of a five-membered ring in oxaporphyrin structures; these O atoms formally have a positive charge. These results are summarized in a decision tree in Fig. 3.

Group A can be re-clustered, revealing further structural information. At a cut-level of 0.75 there are four clusters (AA

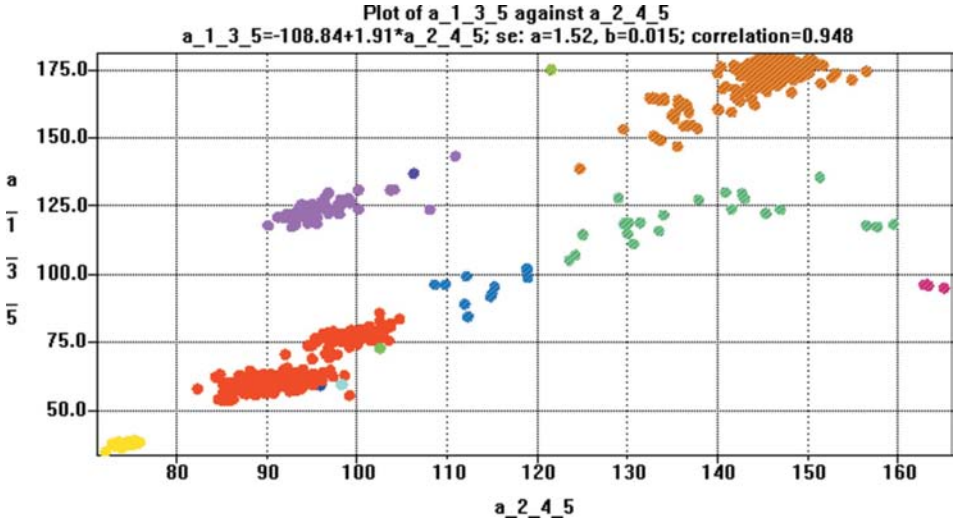

Figure 4
Scatterplot of the C1—C3—C5 angle against the C2—C4—C5 angle (bottom). Sample colours are as in Fig. 2, and taken from the associated dendrogram.

= 1234 fragments; AB = one fragment; AC = three fragments; AD = 133 fragments; see supplementary information[1]). Groups AA and AB correspond to fragments in six-membered rings; in group AB the ring is slightly distorted. Groups AC and AD contain enones constrained to larger rings (see supplementary information).

As well as visual examination of the fragments, the different clusters can be distinguished easily by examining certain interatomic distances and angles. The conformation of the enone can be summarized by the C1—C4 and C2—C5 distances. The former effectively describes the conformation of the C2—C3 double bond as a result of the planarity of the system, and also allows differentiation of different ring sizes, with the largest distances indicating the *trans* configuration, the smallest distances the *cis* form in a five-membered ring. The latter distance indicates the orientation of the C3—C4 single bond, with short distances corresponding to the s-*trans* geometry. Scatterplots show excellent separation of the clusters. Better discrimination is obtained by considering the C1—C3—C5 and C2—C4—C5 angles (see Fig. 4), which combine to describe the geometry.

It is readily seen that these distances and angles are poor at distinguishing the differences between groups A, C, D and E, all of which are *cis* s-*trans*. However, a scatterplot of C3—C4—O6 and C5—C4—O6 angles allows these groups to be separated (see supplementary information). These angles would be expected to conform to standard angles of around 120°, as is the case for the majority of enone fragments, but groups C (green), D (cyan) and E (blue) have markedly small values of one or both of these angles. These structures need to be examined carefully for the possibility of errors in the atomic coordinates (see §5.3.3).

[1] Supplementary data for this paper are available from the IUCr electronic archives (Reference: BK5046). Services for accessing these data are described at the back of the journal.

3.1. Acyclic enones

Cluster analysis was repeated on structures where all the bonds in the carbon backbone of the fragment were defined to be acylic. There were 240 hit structures containing 281 fragments. At a cut level of 0.740, there were five clusters, with a fit of 0.96. These clusters have been designated A′, B′, C′, D′ and E′ to distinguish them from the results of the previous analysis.

Group A′ (52 fragments) contains fragments with a *trans* s-*trans* enone geometry. Groups B′ (221 fragments) and C′ (one fragment) contain fragments with a *trans* s-*cis* enone geometry. In Group C′ (BETNIY) the C3—C4—O6 and C1—C2—C3 angles are larger than in group B′, and this fragment may represent an error in the determination of the position of the O atom (as discussed in §3). Group D′ (four fragments) has enones with a *cis* s-*cis* geometry. In group E′ (three fragments) the enone is non-planar. The C2—C3 bond is *cis*; the oxygen is out of the plane of these atoms, but the C3—C4 bond approaches an s-*cis* geometry. Notably there are no fragments with the *cis* s-*trans* geometry. These results are summarized by the decision tree in Fig. 5 and are used to estimate the energy difference between the various conformers in the solid state, as described in §5.

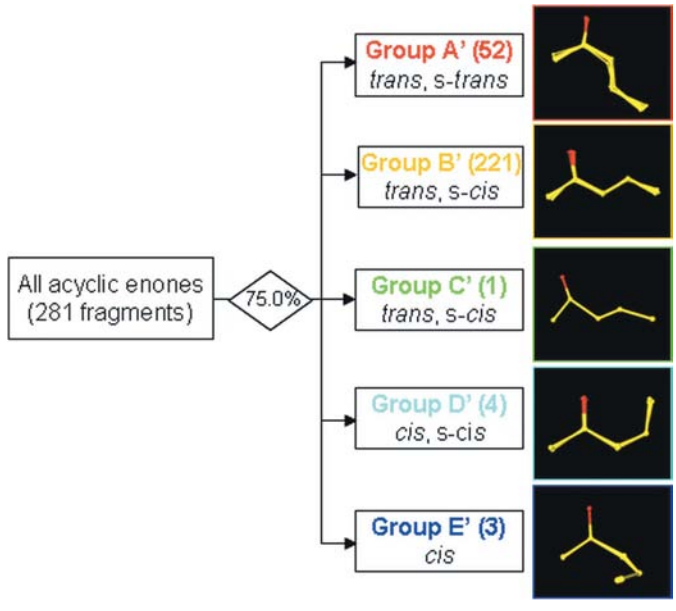

Figure 5
Decision tree for the geometries of acyclic enones.

Table 1
Number of fragments of a given geometry (with the proportion in brackets).

	All enones	Acyclic enones	All enimines
cis s-*cis*	27 (1.5%)	7 (2.5%)	760 (60.7%)
cis s-*trans*	1466 (79.9%)	0 (0%)	411 (32.8%)
trans s-*cis*	266 (14.5%)	222 (79.0%)	19 (1.5%)
trans s-*trans*	76 (4.1%)	52 (18.5%)	63 (5.0%)

3.2. Cyclic enones

When all the bonds in the carbon backbone of the enone are constrained to be cyclic, all the types of groups seen for the initial clustering of the enone are observed, although in a different population ratio. There were 1017 CSD hits yielding 1550 fragments.

At a dendrogram cut-level of 0.835 there are 12 clusters. As for the unconstrained case, the majority of fragments (1458, 94.1%) were of the *cis* s-*trans* conformation. The *trans* s-*cis* conformation, which is the second most common conformation, represents only 2.8% of the dataset (43 fragments). The *trans* s-*trans* conformation accounts for 1.5% (24 fragments) and the *cis* s-*cis* for 1.2% (19 fragments). There are five non-planar fragments (0.3%).

4. Enimine fragment clusterings

Enimines (see Fig. 1*b*) show a similar range of conformations to enones. There are 729 hit structures, yielding 1253 fragments. At a cut-level of 0.750, there are five clusters with a fit of 0.99 (see Fig. 6).

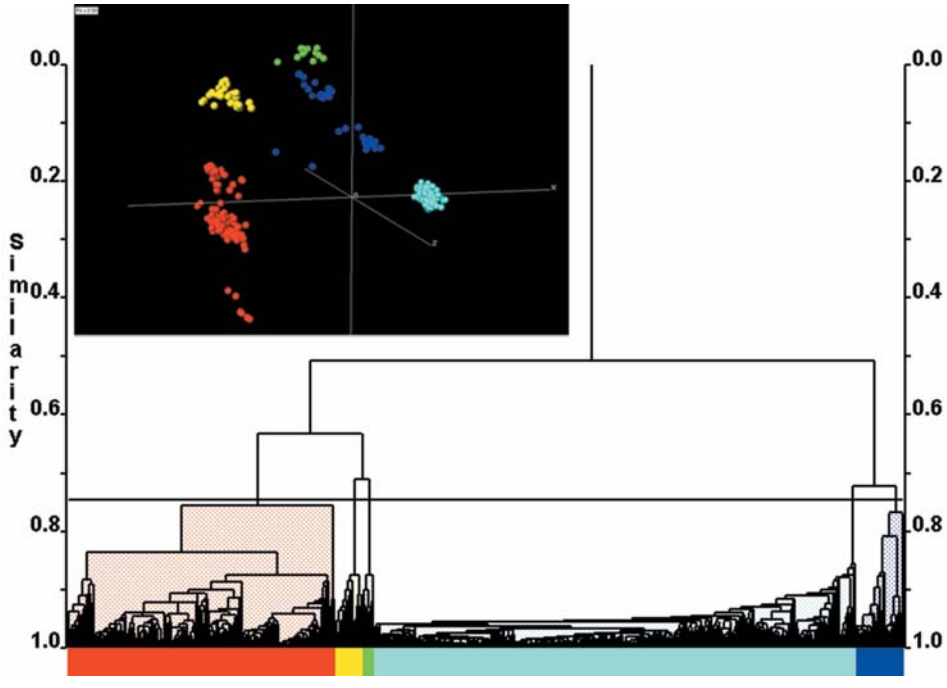

Figure 6
Dendrogram and MMDS plot (inset) for the enimine search fragment.

Cluster A (411 fragments) corresponds to cyclic enimines of the *cis* s-*trans* type, including five-, six- and seven-membered ring structures. From scatterplots comparing interatomic distances and angles, group A appears to have three distinct areas (see Fig. 7) and reclustering group A gives three subclusters at a cut-level of 0.710 with a fit of 0.98 in the MMDS. Group AA (red) corresponds to seven-membered rings, AB (yellow) to six-membered rings and group AC (green) to five-membered rings.

Group B (63 fragments) contains structures of the *trans* s-*trans* type. Group C (19 fragments) contains structures of the *trans* s-*cis* type. Group D (686 fragments) has enimines of the *cis* s-*cis* type, where the N atom forms part of a five-membered ring. The prevalence of this geometry compared with the analogous enone (group L) can be attributed to the large number of porphyrin structures in the CSD, which form a large proportion of group D. Group E (74 fragments) also has enimines of the *cis* s-*cis* type, analogous to group I of the enones. This clustering information is summarized in Fig. 8.

Group E is the most diffuse of the enimine clusters. Reclustering group E gives seven subclusters at a cut level of 0.770, with a fit of 0.99 in the MMDS (see supplemenatry information). All the fragments are of the *cis* s-*cis* configuration, but either of the C1—C4 and C2—O6 distances could be used to differentiate different ring sizes. These measures separate all the subclusters except EA and EC, which differ principally in the C3—C4—C5 angle, which is particularly large for EC. Groups EA, EC (both six-membered rings) and EE (seven-membered rings) are approximately planar. Group EB contains enimines that form part of the seven-membered rings which are part of a fused ring system. Group ED also consists of enimines where the carbon backbone is part of a seven-membered ring. Group EF consists of a fragment where the carbon backbone forms part of a non-planar ten-membered macrocycle. The fragment in Group EG is part of an eight-membered ring.

4.1. Acyclic enimines

There are only 19 structures containing an acyclic enimine in the CSD, yielding 26 fragments for analysis. Such a small number of fragments makes it very difficult to estimate the energy differences between the conformers in the solid state, but nonetheless it does provide a rough comparison, as is shown in §5. At a cut-level of 0.702 there are three clusters with a fit of 0.95 in the MMDS. Groups A (14 fragments) and B (10 fragments) have the *trans* s-*trans* geometry; these differ in the

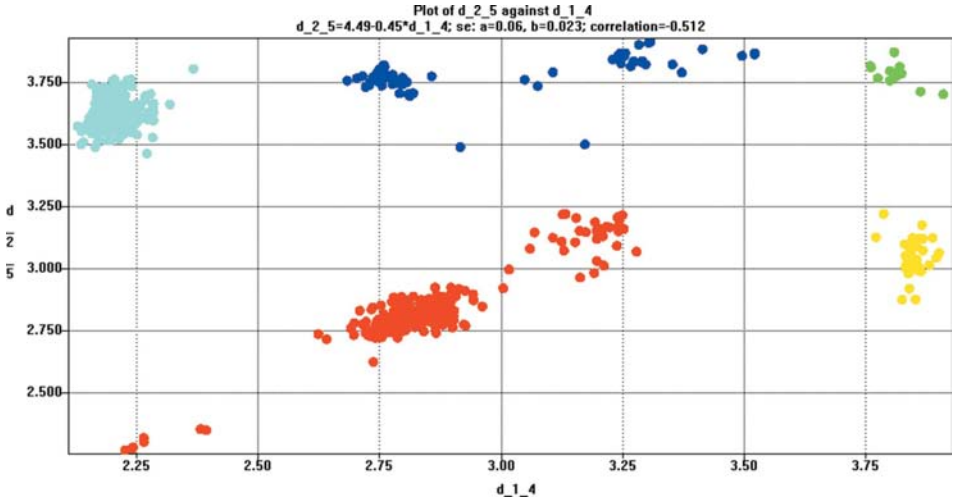

Figure 7
Scatterplot of the C2—C5 distance against C1—C4 distance. Sample colours are as in Fig. 6.

relative position of the N atom, as seen by the smaller C3—C4—O6 and C5—C4—O6 angles of group B than group A. Group C (2 fragments) has the *trans* s-*cis* geometry.

5. Analysis of geometries

5.1. Proportions of different geometry types

In the case of enimines and acylic enones, the different combinations of bond conformation can all be uniquely separated by choice of a suitable cut-level to give four and three clusters, respectively. However, this is not possible for the clustering of all enones.

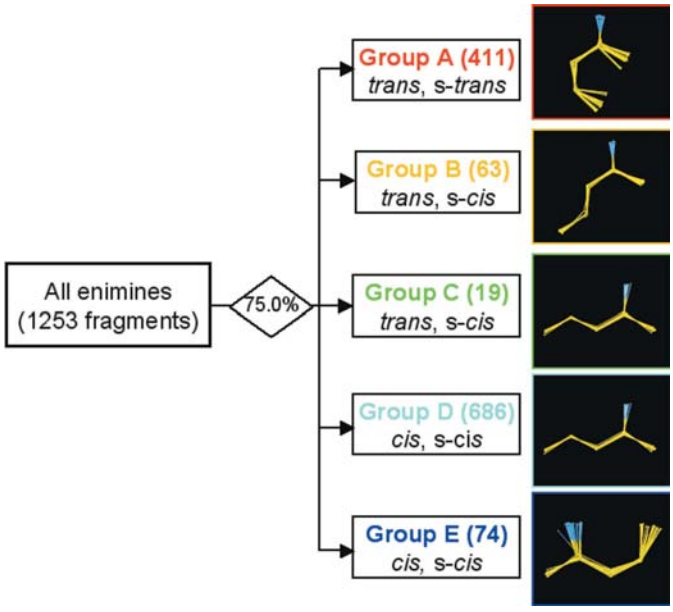

Figure 8
Decision tree for the distribution of enimine geometries.

Apart from the absence of the *cis* s-*trans* geometry in the case of the acyclic enones, the ratio of the remaining geometries is approximately the same as for all enones (see Table 1). However, the distribution of conformation types is quite different between enones and enimines.

The key to these differences in distribution arises because when the N atom has no charge, as is generally the case, it has one other substituent while a neutral O atom will not have any further substituents. This means that in enones the structure can only be propagated through C5, while for enimines the structure can extend through N6 or through C5.

The *cis* s-*cis* configuration is much more prevalent for enimines than for enones; this is largely accounted for by the high number of porphyrin derivatives in the CSD. Steric considerations can be used to rationalize the relatively high frequency of the *trans* s-*trans* geometry for enimines compared with enones. In enones, this occurs when C5 is a terminal methyl group, when the carbon backbone is part of a macrocycle which constrains the geometry, or the substituent on C5 is out of the plane of, and usually perpendicular to, the plane of the enone. The structure rarely propagates through the oxygen. In enimines, the nitrogen can form part of the sterically most demanding substituent, favouring the formation of the *trans* s-*trans* geometry.

5.2. Comparison with computational studies

The relative energies of the four basic forms of but-2-enol have been calculated (Wang *et al.*, 2005) and are ranked from the least to the most stable as *cis* s-*cis* (highest energy), *cis* s-*trans*, *trans* s-*cis*, with *trans* s-*trans* as the most stable form. However, in the aldehyde the s-*trans* form would be expected to be the least sterically hindered, while the s-*cis* would be expected to be the most favoured sterically for the ketone form specified by the CSD search. The *trans* double bond is the most stable for the aldehyde, and this is also expected to be the case in the ketone.

The relative energies of the four principal enone configurations (*cis* s-*cis*, *cis* s-*trans*, *trans* s-*cis* and *trans* s-*trans*) were calculated for pent-2-en-4one (Fig. 9*a*). The forms were optimized using the B3LYP hybrid functional with 6-311++G(d,p) basis sets on all atoms. All calculations were performed with the *GAUSSIAN*03 suite of programs (Frisch *et al.*, 2004). These relative energies were used to calculate the relative occurrences of each of the four geometry types, assuming a simple Boltzmann population distribution and that these four types are the only possible forms. The temperature used was

Table 2
The relative energies and zero-point energies of possible configurations of pent-2-en-4-one.

	Relative electronic energy (kJ mol^{-1})	Relative zero-point energy (kJ mol^{-1})	Calculated proportion of data set (%)	Observed proportion of data set (%)
cis s-*cis*	+8.87	0	1.09	2.49
cis s-*trans*	+18.74	+1.66	0.01	0
trans s-*cis*	0	0	62.58	79.00
trans s-*trans*	+0.69	+0.50	36.33	18.51

Table 3
The relative energies and zero-point energies of possible configurations of 4-penten-2-imine.

	Relative electronic energy (kJ mol^{-1})	Relative zero-point energy (kJ mol^{-1})	Calculated proportion of data set (%)	Observed proportion of data set (%)
cis s-*cis*	+14.09	+0.53	0.08	0
cis s-*trans*	+19.07	+2.31	0.00	0
trans s-*cis*	+6.18	0	6.57	7.69
trans s-*trans*	0	+1.15	93.36	92.31

the average data collection temperature of the dataset (T = 263.2 K, standard deviation = 60.0 K). Only positive frequencies were obtained from the vibrational analyses in each of the optimized molecular structures considered. The results are shown in Table 2.

As discussed above, these calculations can only be compared with the acyclic case. The relative energies of the different geometries lead to the same order in the proportion of each type compared with the observed values (see also Table 1), but *trans* s-*trans* enones are less common and *trans* s-*cis* enones are much more common than predicted by the gas-phase calculations.

Similar calculations were performed on the corresponding enimine, 4-penten-2-imine (see Fig. 9*b*), and these results are shown in Table 3. As for the enone case, the average temperature of the data set was used (T = 227.9 K, standard deviation = 7.39 K), and the vibrational analyses for each of the optimized molecular structures gave only positive frequencies.

Comparing these values to the proportions of acyclic enimines shows that the gas-phase energy calculations are a very good match to the observed conformational ratios found from the cluster analysis in the crystalline solid state, although the number of samples is small in this case.

The gas-phase calculations match well with the observations in the solid state, particularly for the enimine case, where the energy differences between conformers are all large. Differences may arise because the gas phase is not an ideal model for the solid state; this may be especially pertinent to the *trans* s-*cis* and *trans* s-*trans* geometries of the enone fragment, where the energy difference between these geometries is small. Additionally, the 'social bias' in the CSD may influence the results.

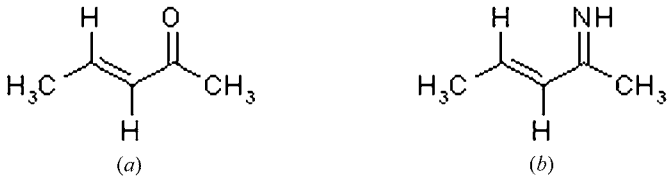

Figure 9
(*a*) Pent-2-en-4-one and (*b*) 4-penten-2-imine used for energy calculations.

5.3. Unusual fragment geometries

Most of the fragments correspond to the four expected cases and are all approximately planar. It is therefore interesting to consider the unusual fragment geometries, where the whole enone or enimine fragment deviates markedly from the plane. In some cases it is apparent from examination of the structure that the deviation from planarity is likely to arise due to misreporting of atomic coordinates.

5.3.1. Non-planar enones. Non-planar enones are not common. For the acyclic case only group E (3 fragments) consists of non-planar enones. It occurs when one or both of the π components of the enone are adjacent to other delocalized systems, *e.g.* BOZETY. In VEVQUI, the non-planarity of the enone fragment appears to arise from steric requirements of other parts of the structure.

5.3.2. Non-planar enimines. Non-planar enimine fragments are mostly found in structures that consist of unusual fused ring systems, which force the non-planar geometry upon the fragment, *e.g.* DAKWER, where the C4═N6 bond forms part of a five-membered ring, while the C2═C3 bond is part of a separate nine-membered ring, and DULDAP, where the N atom is at a bridgehead position and is positively charged. In QUMJAL, the enimine fragment is in a seven-membered ring which is not delocalized.

5.3.3. Possible errors in atomic coordinates of structures in the CSD. Several of the enone fragments discussed in the paper have unusual geometries which appear to be consistent with errors in reporting the atomic coordinates of one or more atoms within the fragment.

BRMOTR (Group C) contains the enone fragment as part of a seven-membered ring. The C5—C4—O6 angle is 105.0°. Comparison with other structures with this ring type suggests that this geometry is not imposed by the ring.

Group D contains two fragments which are present in the structure BNQBRP, in a *p*-benzoquinone molecule. In this structure, the coordinate of the C4 atom appears to be incorrect. As given, the structure has a C═O bond length of 1.570 Å and the C4 atom is out of the plane of the rest of the molecule. Bringing C4 into the plane results in a more reasonable bond length of 1.179 Å (compared with the other C═O bond in the *p*-benzoquinone molecule, which is 1.257 Å). This can be achieved by changing the *y* coordinate of

the atom from −0.214 to −0.14 (in crystal fractions) and is suggestive of a typing error in the recorded atomic coordinates.

XISGIP (group E) is a structure with $Z' = 2$, with the two crystallographically independent molecules related by a pseudo-screw axis. In one of the molecules the C5—C4—O6 angle is 102.5°, while it is 122.1° in the other. This indicates that there is not any intrinsic strain imposed on the enone fragment geometry by the rest of the structure and therefore suggests that there may be an error in the atomic coordinates of one of the molecules.

6. Conclusions

Enones and enimines have a series of well known and expected geometries. Cluster analysis can be used to distinguish these geometries, allowing quantification of the relative likelihoods of each being observed. The analysis can also be used to distinguish outliers, which may highlight unusual or unexpected conformations. Outliers may also arise as a result of errors in determining or reporting a structure. This makes cluster analysis a valuable tool for initial sorting of a dataset prior to study, as it can be used to provide an extra level of filtering of a dataset beyond that offered by *ConQuest*, although the user must be careful to ensure that there are sound, justifiable reasons for excluding any structural fragments. The occurrence of different geometries in acyclic enones and enimines is consistent with the relative energies of four main geometries calculated for 2-penten-4-one and the corresponding enimine.

References

Abraham, R. J. & Lucas, M. S. (1988). *J. Chem. Soc. Perkin Trans. II*, pp. 669–672.

Allen, F. H. (2002). *Acta Cryst.* B**58**, 380–388.

Barr, G., Gilmore, C. J., Parkin, A. & Wilson, C. (2005). *J. Appl. Cryst.* **38**, 833–841.

Bruno, I. J., Cole, J. C., Edgington, P. R., Kessler, M., Macrae, C. F., McCabe, P., Pearson, J. & Taylor, R. (2002). *Acta Cryst.* B**58**, 389–397.

Chamberlin, A. R. & Reich, S. H. (1985). *J. Am. Chem. Soc.* **107**, 1440–1441.

Childs, R. F., Mahendran, M., Blackburn, C. & Antoniadis, G. (1988). *Can. J. Chem.* **66**, 1355–1358.

Frisch, M. J. *et al.* (2004). *GAUSSIAN*03, Revision C.02. Gaussian Inc., Wallingford CT.

Oelichmann, H. J., Bougeard, D. & Schrader, B. (1982*a*). *Angew. Chem.* **94**, 648–649.

Oelichmann, H. J., Bougeard, D. & Schrader, B. (1982*b*). *Angew. Chem.* Suppl., 1404–1415.

Wang, Y.-H., Zou, J.-W., Zhang, B., Lu, Y.-X., Jin, H.-A. & Yu, Q.-S. (2005). *J. Mol. Struct.* **755**, 31–37.